

Study of Radio Transients using COSMOS and STRIPE82 Survey

Drishty B. Jadia
BS-MS Physics
dbjadia05@gmail.com

The COSMOS Deep Survey is a 3 GHz radio survey of the $\sim 2 \text{ deg}^2$ COSMOS field, centered near the celestial equator, conducted with VLA (Very Large Array) telescope covering a bandwidth of 2048 MHz. STRIPE-82 Survey is a 3 GHz VLA survey of the $\sim 270 \text{ deg}^2$ STRIPE-82 region. The project attempts to analyze the data from these surveys, focusing on identifying transient events such as tidal disruption events (TDE), gamma-ray bursts (GRB), and neutron star mergers using imaging and source identification techniques.

I. INTRODUCTION

Astronomical transients are objects that exhibit rapid and significant intensity changes over short timescales, ranging from seconds to years. These events represent extreme physical environments involving high gravity, intense magnetic fields, and extreme velocities and temperatures [1]. These phenomena are crucial in astrophysics as they serve as probes into extreme environments and processes in the universe. Studying radio transients unveils insights into the life cycles of stars, the behavior of compact objects like neutron stars and black holes, and the properties of the interstellar and intergalactic media [2]. They also provide a means to test fundamental physical theories under conditions unattainable on Earth.

Transients can be categorized based on their timescales (shorter or longer than a few seconds) and location (galactic or extra-galactic). Fast Radio Bursts (FRBs) are millisecond-duration flashes of radio waves originating from extragalactic distances, whose origins are still a subject of intense research [3][4]. Pulsars are highly magnetized, rotating neutron stars, that emit radio pulses periodically and serve as precise cosmic clocks [5]. Gamma-Ray Burst (GRB) afterglows are transient emissions following the initial gamma-ray event, providing information about relativistic jet interactions with the surrounding medium [6]. Supernovae and their remnants emit radio waves due to shock interactions with the circumstellar environment [7]. Other categories include X-ray binaries, where variable radio emission arises from accretion processes onto compact objects [8], and Tidal Disruption Events (TDEs), where stars are torn apart by supermassive black holes, leading to transient radio signatures [9][10].

The physical mechanisms driving these transients often involve synchrotron radiation from relativistic particles in magnetic fields, shock interactions with surrounding media, and accretion processes near compact objects. Recent findings highlight the importance of magnetic fields and jet composition in shaping observational characteristics [2][9]. To investigate the underlying physical mechanisms responsible for transient phenomena, I aim to compile and analyze

key source parameters. This study utilizes data from the COSMOS and STRIPE82 fields, both observed with the Karl G. Jansky Very Large Array (VLA). In the previous semester, I focused on the analysis of the COSMOS survey. Currently, my efforts are directed toward automating the calibration and imaging pipeline for the STRIPE82 survey, with the goal of enabling efficient and reproducible data processing.

Section II provides an overview of the COSMOS survey, describing its scope, methodologies, and relevance to the study of radio transients. Section III discusses the STRIPE-82 Survey with a brief of the On-the-Fly Mosaicing mode. Section IV outlines the procedures and analytical techniques employed to achieve the research objectives, offering insight into the data processing and identification of transient events for both the surveys. Section V discusses the progress made in the analysis, and any preliminary interpretations. Finally, Section VI considers future directions for this work, addressing potential improvements, anticipated challenges, and the broader implications of ongoing research in this area.

II. COSMOS 3 GHZ SURVEY

The VLA-COSMOS 3 GHz Deep Project is based on 384 hours of observations with the Karl G. Jansky Very Large Array (VLA) located in New Mexico, USA at 3 GHz (10 cm) with a bandwidth of 2048 MHz, toward the two square degree Cosmic Evolution Survey (COSMOS) field [11]. Radio waves are not obstructed by large clouds of interstellar dust, and Earth's atmosphere is transparent to them, allowing observations in the radio spectrum to be conducted effectively from ground-based telescopes. The observations were taken from November 2012 to January 2013, June to August 2013, and February to May 2013 in A-array (324 hours) and C-array configurations (60 hours) [12]. The VLA-COSMOS Deep Survey data were collected using a grid of 64 pointings, separated by $10'$ in right ascension (RA) and declination (DEC). To achieve a uniform rms sensitivity across $\sim 2 \text{ deg}^2$ field, three sets of these 64 pointings were conducted, resulting in a total of 192 pointings (shown in Figure 3). The first set of pointings is nominal, the second is shifted by

5' in RA and DEC, while the third set is shifted by $-5'$ in RA [12]. We take the reference from [12] for Figure 2 which shows the 1σ sensitivity of each survey as a function of the area covered for past, current, and future radio continuum surveys. We understand that the VLA-Cosmic Evolution Survey (COSMOS) 3 GHz Large Project bridges the gap between past and future radio continuum surveys by covering an area as large as two square degrees down to a sensitivity reached to date only for single pointing observations. This allows for individual detections of $> 10,000$ radio sources. For the MS project, VLA - COSMOS survey is utilised, since it results into the deepest and most sensitive radio images ever produced.

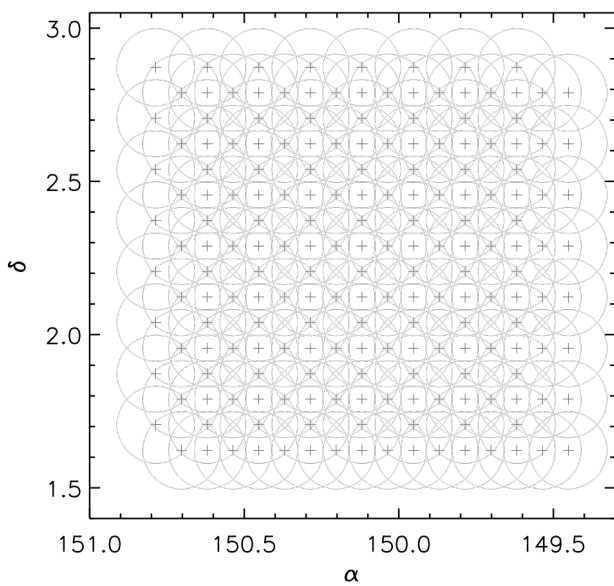


Figure 1. Pointing pattern used for the 3 GHz VLA-COSMOS Large Project. The centers of the 192 pointings are indicated by the plus signs. Circles indicate the primary beam of each pointing.

III. STRIPE-82 SURVEY

The Caltech-NRAO Stripe 82 Survey (CNSS) is benchmark radio transient survey carried out with the Jansky VLA in the Sloan Digital Sky Survey Stripe 82 region at 3 GHz with spectral indices between 2.5 GHz and 3.5 GHz, at a spatial resolution of 3". Stripe 82 is $\sim 270 \text{ deg}^2$ region near the celestial equator. This is the first wide-field survey carried out with the Jansky VLA On-the-Fly Mosaicing (OTFM) mode [13]. The primary goal of the survey is to discover radio transients on timescales of days to years without relying on synoptic surveys at higher frequencies (i.e. optical and X-ray)

OTFM is an observing mode in which the VLA an-

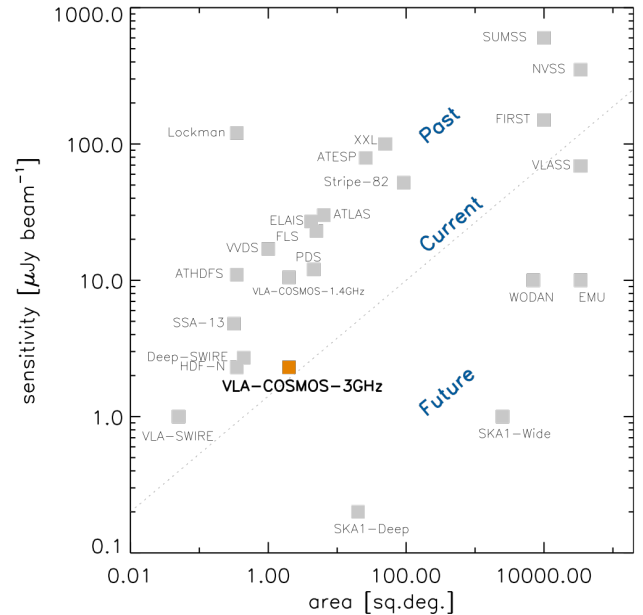


Figure 2. Sensitivity (at the observed frequency of the given survey) vs. area for past, current, and future radio continuum surveys.

tennas continuously move across the sky while collecting data, rather than pointing and settling at discrete sky positions. This is analogous to “on-the-fly mapping” used in single-dish telescopes, adapted for interferometry. Instead of the traditional “point-and-shoot” method where telescopes spend time slewing and settling at each pointing center, OTFM scans smoothly, recording data without stopping, and updates the phase center continuously or at short intervals.

IV. METHODOLOGY

A. COSMOS Survey

The raw data for each set of 64 pointings was obtained from the National Radio Astronomy Observatory (NRAO) Archives. A total of 110 sets corresponding to 110 epochs were downloaded for analysis. The initial step involved calibrating the raw data using an Astronomical Image Processing System (AIPS)-based pipeline [14]. The calibration process included corrections for phase, delay, bandpass, and gain. The raw data files were converted to measurement sets (MS) using the AIPS pipeline. Once processed, the data was imported into the Common Astronomy Software Applications (CASA) [15] for imaging. The imaging process in CASA included initial flagging, self-calibration, and imaging steps. Imaging was performed using the `tclean` task, which is based on the CLEAN algorithm—a widely used method for reconstructing model images from interferometric data.

For imaging, we utilized an image size of 6000×6000 pixels with cell size of $0.2''$. The number of iterations was set to 500 with, `nterms` = 2, and spectral windows (`spw`) 0 and 3 – 12 were employed. A robust parameter of 0.5 was applied, and a primary beam limit of -1 was maintained. The average root mean square (rms) noise for each image obtained was $40\mu Jy$. For pointings where the rms noise exceeded the average, self-calibration was performed using the `gaincal` and `selfcal` tasks to reduce the rms noise.

Following these steps, the resulting image files were visualized using CARTA (Cube Analysis and Rendering Tool for Astronomy) [16]. CARTA was used to inspect the images and verify the effectiveness of the calibration and imaging processes. The images were then converted into FITS files using the CASA task `exportfits`. Subsequently, the FITS files for each pointing were combined to create a mosaic of the entire survey field using AIPS. To prepare the mosaics, the data was loaded into AIPS using the `fitld` task. The `flatn` task was then utilized to create four different mosaics of the COSMOS region. Each mosaic had a size of 18200×18200 pixels, with an rms noise of $60\mu Jy$ per beam. These mosaics provided a comprehensive view of the field (for example shown in Figure 3). In total, we generated 440 mosaics (four mosaics corresponding to each of the 110 epochs).

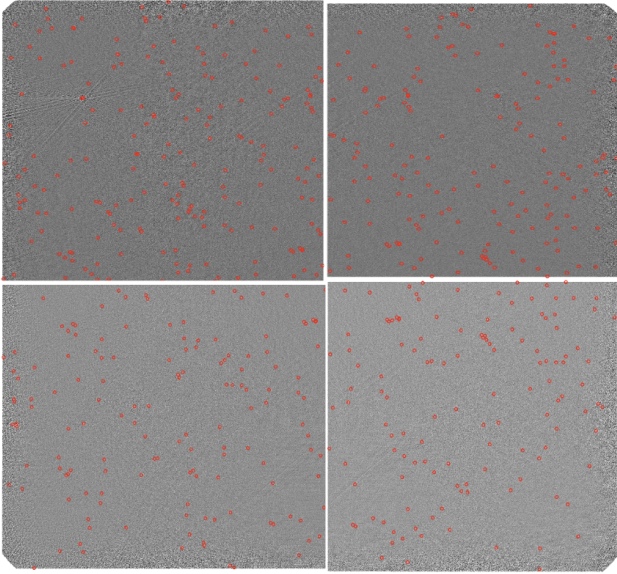


Figure 3. Four Mosaics of one of the datasets. Red circles mark the sources in the corresponding mosaic.

With the mosaics of the COSMOS field prepared, we proceeded to the source finding phase. For source detection and characterization, we analyzed the mosaics using the Python-based source-finding software

PyBDSF (Python Blob Detector and Source Finder) [17]. PyBDSF is designed to identify and catalog astronomical sources in radio interferometric images. The source finding was performed using the `process_image` task, which scans the mosaics to detect sources based on predefined criteria such as signal-to-noise ratio and morphological parameters. The resulting source catalogs were obtained in CSV format using the `write_catalog` function, providing a structured dataset of detected sources for subsequent analysis.

B. STRIPE-82 Survey

STRIPE-82 Survey is done through On-the-Fly Mosaicing mode, unlike pointings in COSMOS Survey. For this survey, we want to automate the calibration process. I used the VLASS (VLA Sky Survey) pipeline to perform the calibration of the data. VLASS pipeline primarily uses the standard VLA calibration pipeline but with the sky survey recipe. The pipeline takes roughly 20-24 hrs to run on one dataset depending upon its size. I utilised the NRAO servers facility to run the pipeline effectively.

The pipeline performs the following tasks in order:

1. `hifv_importdata(vis=vislist)` imports raw VLASS MS file into CASA environment;
2. `hifv_hanning()` Hanning-smooths the MS. This procedure reduces the Gibbs phenomenon (ringing) when extremely bright and narrow spectral features are present and spill over into adjacent spectral channels.
3. `hifv_flagdata(...)` Flags data from scans with known bad intents such as pointing, focus, or system problems. Also, flags autocorrelations, shadowed antennas, and edge SPWs (if configured).
4. `hifv_vlasetjy()` calculates and sets the spectral and spatial model of the calibrator for the standard VLA flux density calibrators. It also plots the amplitude versus uv-distance for the models per spw that are calculated and used to specify the flux density calibrator characteristics.
5. `hifv_priorcal(...)` applies antenna position corrections, gain curve and opacity corrections and requantizer gain corrections.
6. `hifv_syspower()` uses system temperature and power data to improve calibration weights.
7. `hifv_testBPDcal(...)` performs initial bandpass and delay calibration on suitable calibrators.
8. `hifv_checkflag(checkflagmode='bpd-vlass')` uses the `rflag` algorithm to flag RFI in bandpass calibrator data.

9. `hifv_finalcals()` applies all gain, bandpass, and delay corrections to produce final tables.

10. `hifv_applycals(...)` applies all calibration tables to the data.

After the pipeline has completed its run, the next step is to verify the output to ensure that all tasks were executed successfully. This involves examining the generated plots and flagging summaries to check for any issues. If any tasks failed, I investigate the error messages and logs to identify the cause and debug the problem accordingly.

The next step is to perform imaging of the data. Since the observations were taken in OTFM (On-The-Fly Mapping) mode, we will not use the standard imaging pipeline. Instead, we will carry out the imaging manually using the `tclean` task to have more control over the process.

It is important to note that this is the first time calibration and imaging are being carried out for the CNSS data. As a result, the process involves significant exploration and experimentation to identify the most effective approach, making it a time-consuming but crucial part of the project.

V. WORK PROGRESS

Throughout the course of both the semesters, we have made significant progress in processing the data from the VLA COSMOS 3GHz survey and STRIPE-82 Survey. We successfully produced mosaics for 80 epochs out of 110 epochs, resulting in a total of 320 mosaics that are now ready for source finding. The substantial size of each mosaic FITS file, approximately 1.3 GB, means that the source-finding process using PyBDSF is computationally intensive and time-consuming for each mosaic. Consequently, completing the source finding for all mosaics requires additional time and computational resources. We have done source finding on all 320 mosaics. In any particular mosaic, we got a total of 612 sources by doing source finding. For the calibration of the remaining 30 epochs, we generated a CASA-based script due to the failure of the AIPSLite-based pipeline. This CASA script includes gain, delay, phase, bandpass, flux, and amplitude calibration. Currently, we are processing these 30 epochs with the script. After processing all, we will repeat the process we did for 80 epochs. Here I present a subset of a csv output file of one mosaic (shown in Table I).

As part of my ongoing work on the STRIPE82 survey, I have successfully executed the VLASS calibration pipeline on the relevant datasets. Following this, I am currently working on implementing a manual imaging procedure. This stage is particularly challenging and

| Isl id | RA | DEC | Total Flux | Peak Flux |
|--------|-----------|---------|------------|-----------|
| 0 | 150.78619 | 2.09865 | 0.00060642 | 0.0005153 |
| 1 | 150.78627 | 2.45638 | 0.00075763 | 0.0004794 |
| 2 | 150.78631 | 2.90398 | 0.00240459 | 0.0015069 |
| 3 | 150.78632 | 2.91497 | 0.00270052 | 0.0013034 |
| 4 | 150.78612 | 2.15630 | 0.00039446 | 0.0022756 |

Table I. A subset of a CSV output file for one of the VLA COSMOS 3GHz survey mosaics, showing source properties.

time-intensive due to the survey being conducted in On-The-Fly Mapping (OTFM) mode, which complicates the imaging process compared to traditional pointing observations.

A critical aspect of this step involves determining whether primary beam correction is required for our specific data, which demands a careful examination of the observation setup and calibration outcomes. Moreover, the existing imaging scripts utilizing `tclean` are poorly structured and insufficient for our needs. As a result, I am in the process of developing a custom imaging script tailored to the STRIPE82 dataset. This effort requires extensive testing, optimization, and validation, making it a considerably time-consuming but essential part of the project.

VI. FUTURE SCOPE

Even after the completion of my semester, I intend to continue working on my project. We have done source finding on all 320 mosaics and made light curves correspond to these sources. Upon completing the source finding on the remaining 120 mosaics, which we are making now, the next step will involve cross-matching the detected sources across all epochs to construct light curves for each source. This will enable a comprehensive variability analysis of the sources across the multiple epochs. By examining the variability patterns, we aim to identify transient activity, if present, in the detected sources. This analysis will contribute to understanding the nature and behavior of potential transient phenomena within the COSMOS field.

For STRIPE-82 survey, the future work will focus on finalizing and validating the custom imaging script to ensure it produces reliable and high-quality images for the STRIPE82 dataset. Once the manual imaging workflow is established, I will proceed with primary beam correction (if required) and mosaicking of the individual pointings to generate a uniform and continuous image of the survey region.

The next steps involve completing and validating the custom imaging script, followed by primary beam correc-

tion and mosaicking. I will then perform source finding, cross-match sources across epochs to identify transients

and variables, and analyze their properties to investigate the underlying physical mechanisms.

-
- [1] J. M. Cordes, T. J. W. Lazio, and M. McLaughlin, *New Astronomy Reviews* **48**, 1459 (2004), science with the Square Kilometre Array.
- [2] R. P. Fender and M. E. Bell, “Radio transients: An antediluvian review,” (2011), [arXiv:1112.2579 \[astro-ph.HE\]](#).
- [3] J. M. Cordes and S. Chatterjee, **57**, 417 (2019), [arXiv:1906.05878 \[astro-ph.HE\]](#).
- [4] D. R. Lorimer, M. Bailes, M. A. McLaughlin, D. J. Narkevic, and F. Crawford, *Science* **318**, 777 (2007), [arXiv:0709.4301 \[astro-ph\]](#).
- [5] Stappers, B. W., Hessels, J. W. T., Alexov, A., Anderson, K., Coenen, T., Hassall, T., Karastergiou, A., Kondratiev, V. I., Kramer, M., van Leeuwen, J., Mol, J. D., Noutsos, A., Romein, J. W., Weltevrede, P., Fender, R., Wijers, R. A. M. J., Bähren, L., Bell, M. E., Broderick, J., Daw, E. J., Dhillon, V. S., Eislöffel, J., Falcke, H., Griessmeier, J., Law, C., Markoff, S., Miller-Jones, J. C. A., Scheers, B., Spreeuw, H., Swinbank, J., ter Veen, S., Wise, M. W., Wucknitz, O., Zarka, P., Anderson, J., Asgekar, A., Avruch, I. M., Beck, R., Bannema, P., Bentum, M. J., Best, P., Bregman, J., Brentjens, M., van de Brink, R. H., Broekema, P. C., Brouw, W. N., Brüggem, M., de Bruyn, A. G., Butcher, H. R., Ciardi, B., Conway, J., Dettmar, R.-J., van Duin, A., van Enst, J., Garrett, M., Gerbers, M., Grit, T., Gunst, A., van Haarlem, M. P., Hamaker, J. P., Heald, G., Hoeft, M., Holties, H., Horneffer, A., Koopmans, L. V. E., Kuper, G., Loose, M., Maat, P., McKay-Bukowski, D., McKean, J. P., Miley, G., Morganti, R., Nijboer, R., Noordam, J. E., Norden, M., Olofsson, H., Pandey-Pommier, M., Polatidis, A., Reich, W., Röttgering, H., Schoenmakers, A., Sluman, J., Smirnov, O., Steinmetz, M., Sterks, C. G. M., Tagger, M., Tang, Y., Vermeulen, R., Vermaas, N., Vogt, C., de Vos, M., Wijnholds, S. J., Yatawatta, S., and Zensus, A., *AA* **530**, A80 (2011).
- [6] P. Mészáros, *Reports on Progress in Physics* **69**, 2259 (2006).
- [7] D. A. Frail, S. R. Kulkarni, E. O. Ofek, G. C. Bower, and E. Nakar, *The Astrophysical Journal* **747**, 70 (2012).
- [8] B. E. Tetarenko, G. R. Sivakoff, C. O. Heinke, and J. C. Gladstone, *The Astrophysical Journal Supplement Series* **222**, 15 (2016).
- [9] K. D. Alexander, S. van Velzen, A. Horesh, and B. A. Zauderer, *Space Science Reviews* **216**, 81 (2020).
- [10] K. D. Alexander, M. H. Wieringa, E. Berger, R. D. Saxton, and S. Komossa, *The Astrophysical Journal* **837**, 153 (2017).
- [11] Smolčić, V., Delvecchio, I., Zamorani, G., Baran, N., Novak, M., Delhaize, J., Schinnerer, E., Berta, S., Bondi, M., Ciliegi, P., Capak, P., Civano, F., Karim, A., Le Fevre, O., Ilbert, O., Laigle, C., Marchesi, S., McCracken, H. J., Tasca, L., Salvato, M., and Vardoulaki, E., *AA* **602**, A2 (2017).
- [12] V. Smolčić, M. Novak, M. Bondi, P. Ciliegi, K. P. Mooley, E. Schinnerer, G. Zamorani, F. Navarrete, S. Bourke, A. Karim, E. Vardoulaki, S. Leslie, J. Delhaize, C. L. Carilli, S. T. Myers, N. Baran, I. Delvecchio, O. Miettinen, J. Banfield, M. Baloković, F. Bertoldi, P. Capak, D. A. Frail, G. Hallinan, H. Hao, N. Herrera Ruiz, A. Horesh, O. Ilbert, H. Intema, V. Jelić, H.-R. Klöckner, J. Krpan, S. R. Kulkarni, H. McCracken, C. Laigle, E. Middleberg, E. J. Murphy, M. Sargent, N. Z. Scoville, and K. Sheth, *Astronomy and Astrophysics* **602**, A1 (2017).
- [13] K. P. Mooley, S. T. Myers, D. A. Frail, G. Hallinan, B. Butler, A. Kimball, and K. Golap, *The Astrophysical Journal* **870**, 25 (2018).
- [14] E. W. Greisen, in *Acquisition, Processing and Archiving of Astronomical Images*, edited by G. Longo and G. Sedmak (1990) pp. 125–142.
- [15] T. C. Team, B. Bean, S. Bhatnagar, S. Castro, J. D. Meyer, B. Emonts, E. Garcia, R. Garwood, K. Golap, J. G. Villalba, P. Harris, Y. Hayashi, J. Hoskins, M. Hsieh, P. Jagannathan, W. Kawasaki, A. Keimpema, M. Kettenis, J. Lopez, J. Marvil, J. Masters, A. McNichols, D. Mehringer, R. Miel, G. Moellenbrock, F. Montesino, T. Nakazato, J. Ott, D. Petry, M. Pokorny, R. Raba, U. Rau, D. Schiebel, N. Schweighart, S. Sekhar, K. Shimada, D. Small, J.-W. Steeb, K. Sugimoto, V. Suoranta, T. Tsutsumi, I. M. van Bemmelen, M. Verkouter, A. Wells, W. Xiong, A. Szomoru, M. Griffith, B. Glendenning, and J. Kern, *Publications of the Astronomical Society of the Pacific* **134**, 114501 (2022).
- [16] A. Comrie, K.-S. Wang, Y.-H. Hwang, A. Moraghan, P. Harris, A. Pińska, C. Raul-Omar, C.-C. Chiang, M.-Y. Lin, T.-H. Chang, and R. Simmonds, “Carta: The cube analysis and rendering tool for astronomy,” (2024).
- [17] N. Mohan and D. Rafferty, “PyBDSF: Python Blob Detection and Source Finder,” *Astrophysics Source Code Library*, record ascl:1502.007 (2015).